



# A new Earth Observation–based WRF configuration for urban regional climate simulations over Paris

Iraklis Kyriakidis<sup>1</sup>, Vasileios Pavlidis<sup>1</sup>, Maria Gkolemi<sup>2</sup>, Zina Mitraka<sup>2</sup>, Nektarios Chrysoulakis<sup>2</sup>, Josipa Milovac<sup>3</sup>, Jesus Fernandez<sup>3</sup>, Eleni Katragkou<sup>1</sup>

5 <sup>1</sup>Department of Meteorology and Climatology, School of Geology, Aristotle University of Thessaloniki, Thessaloniki, 54124, Greece

<sup>2</sup>Remote Sensing Lab, Foundation for Research and Technology – Hellas, Heraklion, 70013, Greece

<sup>3</sup>Instituto de Fisica de Cantabria (IFCA), CSIC-Universidad de Cantabria, Santander, 39005, Spain

10 *Correspondence to:* Iraklis Kyriakidis (ikyrid@geo.auth.gr)

## Abstract.

In this study, Earth Observation (EO) data describing urban morphology and thermal properties are used to configure the urban representation of Paris in the Weather Research and Forecasting (WRF) model. Model performance is assessed in convective permitting simulations (3 km) in three configurations covering summer 2020: (i) a baseline simulation employing a bulk parameterization of urban areas (i.e. BULK); (ii) a simulation using the BEP–BEM urban canopy model with default urban parameter values (CTRL); and (iii) a simulation in which the BEP–BEM urban canopy parameters are specifically adapted to Paris using EO–derived information (PAR). Comparison with observations from the Météo–France RADOME meteorological network indicates that the BULK simulation produces a systematic warm bias, with a persistent overestimation of nighttime temperatures. Coupling of the urban canopy model leads to an improved overall model performance relative to the BULK configuration for summer–mean conditions. Both BEP–BEM simulations are comparable, with the best performance during summer daytime achieved for the CTRL (0.93 °C lower bias compared to BULK) and during summer nighttime for the PAR simulation (0.22 °C lower bias compared to BULK) over urban grid cells. Over non–urban grid cells, the best performance is exhibited for the PAR simulation with a summer daytime bias of -0.26 °C and a summer nighttime bias of 1.62 °C. The simulated urban–rural temperature contrast for both BEP–BEM simulations is improved compared to BULK, resulting in a more realistic representation of the Urban Heat Island (UHI). Applying the Local Climate Zones (LCZ) classification, which accounts for intraurban differences in urban form and land cover, an analysis was conducted for each urban–type LCZ class present within the Paris urban area, linking each urban station to its nearest LCZ grid cell, enabling station–based comparisons by urban–type LCZ category. This analysis indicates that the PAR configuration better captures spatial urban temperature variability, reflecting the differences in urban forcing introduced by the EO data. During the heatwave of August 2020, the model – regardless of the configuration – becomes warmer and particularly over the urbanized LCZs. The PAR simulation exhibits pronounced temperature overestimations in the city center, due to the methodology adopted for EO data implementation and the selection of the area from which the EO data were derived, leading to urban characteristics which intensified heat storage and trapping. Non–urban areas are better simulated in both BEP–BEM simulations compared to the



35 BULK. Our results demonstrate the added value of a) the coupling of an urban canopy model to WRF and b) the city-tailored configuration of urban canopy morphological parameters in convection-permitting regional climate simulations. The PAR experiment further illustrates the potential of EO-derived datasets to inform urban canopy parameter configurations, enabling a more detailed representation of the urban form and improved simulation of UHI characteristics.

## 1 Introduction

40 The world has become increasingly more urbanized, and projections indicate that two-thirds of the growth of the world's population between now and 2050 will take place in cities (United Nations, 2025). Urban areas influence climate across multiple spatial scales, ranging from the street up to the city, regional and global scale (Britter and Hanna, 2003). The continuing trend of urbanization substantially modifies the urban environment, thereby affecting urban biogeophysical and atmospheric chemical processes and generating numerous feedbacks on weather and, in turn, regional climate. To be able to  
45 forecast and project such interactions between urban environments and local to regional climate, particularly in the context of a changing climate, it is essential to develop tools that realistically represent urban-scale processes via urban parameterizations integrated in cross-scale atmospheric models. This is not a trivial task, as urban areas and urban dynamics are extensively complex. They consist of buildings and impervious surfaces with specific radiative and thermal properties as well as complex three-dimensional morphologies (e.g. building heights, roof and road widths). Urban environments also include anthropogenic  
50 activities and heterogeneous green/blue spaces that further alter energy and water fluxes. Together, these factors create a unique and highly challenging system to understand, simulate and project.

Currently, the Coupled Model Intercomparison Project (CMIP) protocols represent urban environments in a homogeneous manner, with limited differentiation among cities. Moreover, the spatial resolution of climate simulations, typically coarser than 50 km for global models and 12 km for regional models, does not allow for explicit identification of urban land uses or  
55 the adequate representation of urban-scale processes. Recognizing the importance of understanding the impact of urban environment on climate, a Flagship Pilot Study on Urban Environment and Regional Climate Change (FPS URB-RCC) was initiated within the framework of the World Climate Research Programme – Coordinated Regional Climate Downscaling Experiment (WCRP-CORDEX) community (Langendijk et al., 2024). The aim of this initiative is to coordinate and produce a high resolution (~ 3 km) ensemble of urban regional climate simulations under a common protocol, perform robust analyses  
60 and provide valuable insights to the urban climate research community.

This study presents a comprehensive evaluation of a simplified and a more sophisticated representation of urban processes in WRF, the latter through the the Building Effect Parameterization (BEP) coupled with a Building Energy Model (BEM) (Martilli et al., 2002; Salamanca et al., 2010; Salamanca and Martilli, 2010), which uses as input urban canopy parameters (UCPs). Although default UCP values are available in WRF, they can also be derived from EO data, enabling their modification



65 in order to be tailored to a specific area of interest (AOI). While the FPS URB–RCC simulation protocol is closely followed,  
the key novelty of this work is the use of an EO–based dataset, employed to parameterize the distinctive urban characteristics  
of the AOI, which is the city of Paris. This approach enables an assessment of whether city–specific urban features based on  
EO data exert a significant influence on regional climate simulations and whether they can provide more accurate climate data  
and city–scale information. In the following sections we present the methodology followed to collect and process the EO data  
70 for Paris, describe their implementation within the Weather Research and Forecasting (WRF) regional climate model and  
evaluate model performance over the Paris region for three different urban model configurations.

## 2 Data & Methodology

### 2.1 WRF model configuration and physics

The WRF v4.5.1 (Skamarock et al., 2021) model configured in accordance with the CORDEX FPS URB–RCC (Langendijk  
75 et al., 2024). was employed in this study. The main physical parameterization schemes used in the simulations are summarized  
in Table 1. The model setup consists of a two–domain configuration. The parent domain (d01) covers Europe at a horizontal  
resolution of 12 km, following the EURO–CORDEX (Jacob et al., 2020) domain size, with a one–way nested inner domain  
centred over the greater Paris region with a horizontal resolution of 3 km (Figure 1). Convection is explicitly resolved in the  
inner domain (d02); therefore, no cumulus parameterization scheme is applied at the 3 km resolution. The vertical discretization  
80 includes 60 terrain–following sigma levels, with enhanced resolution within the planetary boundary layer to better represent  
near–surface processes. All simulations are driven by the ECMWF ERA5 reanalysis dataset (Hersbach et al., 2020) at a  
horizontal resolution of  $0.25^\circ \times 0.25^\circ$  and 6–hourly temporal intervals. Each simulation was initialized on 1 March 2020 and  
integrated for a total period of six months, covering March through August 2020. The initial two months (March and April  
2020) were discarded as spin–up period.

85 **Table 1:** Parameterizations used for all WRF simulations.

Land Surface Model	Noah–MP (Niu et al., 2011; Yang et al., 2011)
Planetary Boundary Layer (PBL) Scheme	BouLac (Bougeault and Lacarrere, 1989)
Microphysics	Thompson (Thompson et al., 2004, 2008)
Long– and Short–wave radiation	RRTMG (Iacono et al., 2008)
Cumulus parameterization (only for d01)	Kain–Fritsch (KF) (Kain, 2004)
Shallow convection scheme (only for d02)	GRIMS (Hong and Jang, 2018)

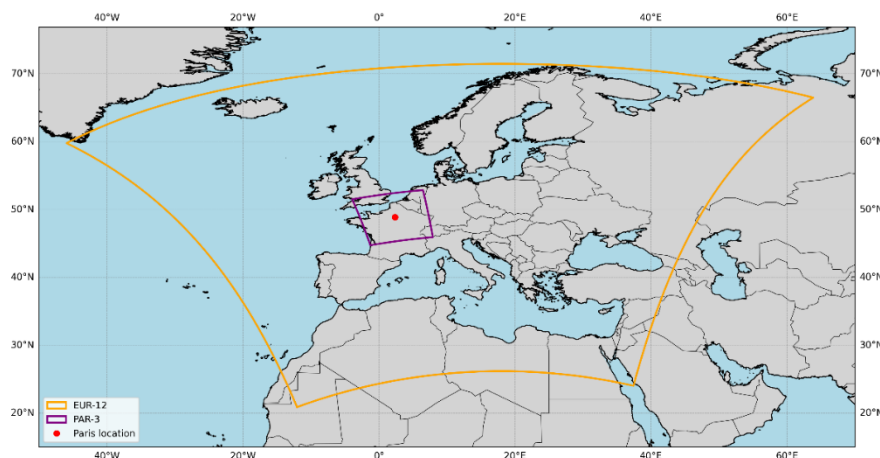


**Figure 1: Domain configuration. EUR-12 (coloured yellow) represents the outer d01 domain. PAR-3 (coloured purple) represents the inner d02 domain, while red dot points to Paris.**

## 90 2.2 WRF urban physics

The WRF model provides a variety of options for representing urban environments. The simplest and default option is the BULK approach (i.e. urban parameterization switched off). In this approach, which is integrated inside WRF's any given land surface model (LSM), all grid cells classified as urban are assigned generic urban properties (e.g. roughness length, surface albedo, heat capacity, thermal conductivity) without reference to the specific characteristics of a simulated city. Under this approach, parameters are modified for urban grid cells to better account for the zero-order effects of urban surfaces, particularly with respect to wind speed and heat storage capacity (Chen et al., 2011; Liu et al., 2006).

Further efforts to improve the representation of urban areas and the processes that occur within them have led to the coupling of different urban canopy models (UCMs) with LSMs of WRF. This coupling involves activating UCMs for the urban fraction within urban grid cells only, replacing the land surface model for this fraction when computing fluxes (e.g. heat and momentum). The LSMs compute these fluxes for the remaining non-urban fraction. The final fluxes are area-weighted and averaged for the entire cell.

The single-layer urban canopy model (SLUCM) and the building effect parameterization (BEP) represent the thermal and momentum exchanges between the urban canopy and the overlying atmosphere using, respectively, a single- and multi-layer model grid. Thus, SLUCM (sf\_urban\_physics=1) consists of two-dimensional, symmetrical street canyons with infinite length and a simplified geometry of the urban canopy, while the radiation treatment is three-dimensional, since it includes both the canyon orientation and the diurnal variation of solar azimuth angle (Kusaka et al., 2001; Kusaka and Kimura, 2004). The scheme neglects the variation in building height within each urban land use category. BEP (sf\_urban\_physics=2), on the other hand, parameterizes a three-dimensional urban morphology within a multi-layer framework, enabling variations in building heights and building density, defined by the road widths in urban grid cells (Martilli et al., 2002). In this way, the vertical



110 distribution of sources and sinks of heat, moisture and momentum induced by buildings is explicitly represented, which shapes  
the thermodynamic profile of the urban roughness sub-layer and, consequently, the urban boundary layer, in more detail than  
SLUCM.

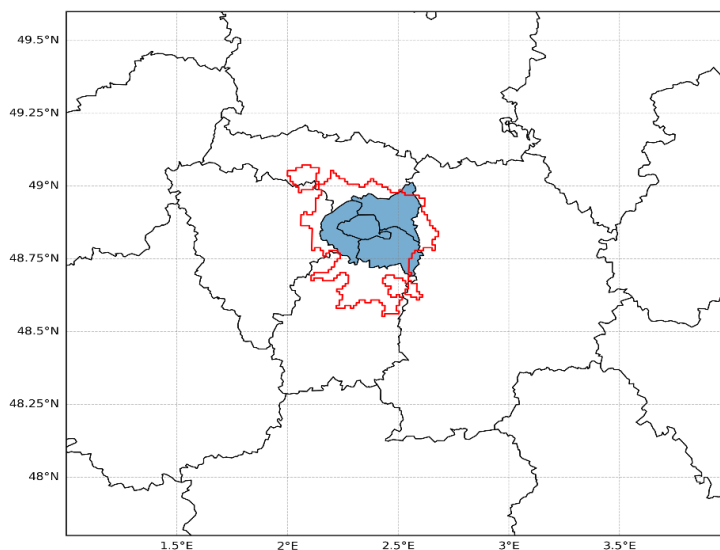
In this work we focus on the most sophisticated UCM available in WRF (`sf_urban_physics=3`). BEP, coupled to a building  
energy model (BEP-BEM), simulates in more detail the local urban processes, energy consumption and the urban heat island  
115 (UHI) effect by incorporating building morphology and anthropogenic heat release. The BEM component estimates  
anthropogenic heat emissions from air conditioning and heating systems and simulates heat exchanges between building  
interiors and the surrounding atmosphere, thereby representing the functional aspects of the urban environment (Salamanca et  
al., 2010; Salamanca and Martilli, 2010). Given the complexity of this urban scheme, its functionality is dependent on a variety  
of urban canopy parameters (UCPs) that are integrated into WRF. Thus, BEP-BEM uses as input UCPs with default values  
120 through predefined tables (`URBPARAM_LCZ.TBL`), based on the World Urban Database and Access Portal Tools (WUDAPT)  
Local Climate Zones (LCZ) (Brousse et al., 2016; Ching et al., 2018; Martilli et al., 2016) that capture aspects of 1)  
morphological, 2) thermal and 3) human related parameters. The first two categories describe the physical form of the urban  
environment, while the latter represents its functional characteristics. All these parameters can be modified to user-set values.

Until recently, each urban canopy parameter was assigned a default value based on the LCZ classification (Stewart and Oke,  
125 2012). In short, this classification system defines 17 land cover types, of which 10 are urban (built type) classes, primarily  
based on building height (high-rise, mid-rise, low-rise) and building density (dense, open, sparse). Within WRF it is assumed  
that neighborhoods with similar form and land cover produce similar local UHI effects and exhibit relatively homogeneous  
temperatures compared with other LCZs. Each LCZ also has predefined values concerning physical and thermal properties,  
based on measurements. However, these default values can become unrealistic for European cities, given the heterogeneity of  
130 European urban structures. Starting from WRF v4.6.0, an updated lookup table with more representative values is introduced  
as default in WRF.

In this study, to better exploit the capabilities of the LCZ-based parameterization and to achieve a more realistic representation  
of the area of interest, all morphological parameters and a subset of the thermal parameters were updated in the lookup table  
for each LCZ class, using urban characteristics specifically tailored to the Paris region. This reference area used to construct  
135 the tailored dataset cover the city of Paris and its three adjacent departments: Seine-Saint-Denis, Val-de-Marne, and Hauts-  
de-Seine. It should be noted that these departments encompass only a part of the broader Paris metropolitan area, as the urban  
agglomeration extends well beyond these administrative boundaries, based on the Global Human Settlement Urban Database  
(GHS-UCDB) polygons delimiting urban areas (Florczyk et al., 2015), depicted in Figure 2. Moreover, we must note that any  
changes in the LCZ UCP lookup table affected all LCZ grid cells throughout the inner domain in its entirety and not only the  
140 Paris region, even though the EO-derived UCP values were obtained using the reference area. Additionally, UCPs related to



anthropogenic urban heat emissions remained unchanged from the default values WRF provides and were assumed to be constant over 24 hours.



145 **Figure 2: Districts that were used (coloured blue) as a reference area for the urban form parameters tailored for Paris region. Red polygon the urban area of Paris, according to the GHS–UCDB polygons delimiting urban areas.**

### 2.2.1 Urban canopy parameters derived from EO data

The tailored urban parameters used as input to WRF’s BEP–BEM UCM were derived from high spatial resolution Earth Observation data, including satellite data (i.e. Sentinel-2, ECOSTRESS), Copernicus Services data (notably the Copernicus Land Monitoring Service Urban Atlas) and available cadastral data from the city of Paris.

150 First, the urban parameters were computed at high spatial resolution (ranging from 1 m to 100 m depending on the data source). These parameters were then aggregated to derive representative values for each LCZ at a spatial resolution of 100 m, following the methodology of Demuzere et al., (2022). Subsequently, these LCZ–based parameters were further aggregated to match the horizontal resolution of the inner WRF domain (3 km) and implemented into the LCZ–lookup table for each urban class.

155 The parameters modified within WRF include: 1) building height, 2) building width, 3) road width, 4) urban fraction, 5) surface albedo of building wall, 6) surface albedo of roof, 7) surface albedo of road, 8) surface emissivity of building wall, 9) surface emissivity of roof and 10) surface emissivity of road. Details of the updated values from the EO data and those used as default in WRF4.6.0 for the abovementioned UCPs are shared in supplementary material (Tables S1 and S2). The EO data–driven values indicate a more urbanized environment than the default table, as for the majority of the LCZs the buildings are denser, wider and with increased height values, with height distribution shifted towards taller buildings. Note that three LCZ classes



160 are not included in Paris area, namely: Compact Highrise (LCZ1), Lightweight low-rise (LCZ7) and Heavy Industry (LCZ10).  
Hence, for these three LCZs the values of the UCPs were not updated and therefore remained the same for all the simulations  
using the BEP-BEM urban parameterization.

### 2.3 Land Use Data

165 In all simulations we employed the high-resolution land use and land cover dataset for regional climate modeling (Reinhart et  
al., 2022; Hoffmann et al., 2023) as described in the EURO-CORDEX simulation protocol (Katragkou et al., 2024). The land  
use and land cover information was held fixed at conditions representative of the year 2015, in accordance with the design of  
all evaluation runs within the EURO-CORDEX experiment.

For the simulation employing the BULK approach, category 13 (“Urban and Built-Up”) of the International Geosphere-  
Biosphere Programme – Moderate Resolution Image Spectroradiometer (IGBP MODIS) classification was assigned to all  
170 urban cells, as the BULK approach does not support differentiation of urban areas into multiple land use and physical property  
classes such as LCZs. Figure 3a illustrates the land use representation for domain d02.

For the simulations employing the BEP-BEM UCM, urban areas are represented using the 10 urban (built type) classes from  
the WUDAPT LCZ classification (Brousse et al., 2016; Ching et al., 2018; Martilli et al., 2016), with the inclusion of the “Bare  
rock or paved” category, interpreted as asphalt and aligned with LCZ land cover type E. For non-urban grid cells, the model  
175 applies the modified IGBP MODIS land cover classification, which distinguishes 20 land cover types (codes 1 to 20).  
Compared to the single “Urban and Built-Up” category (IGBP MODIS category 13), this approach provides substantially  
greater detail and discretization of urban land use, thereby enhancing the representation of urban heterogeneity within the  
model. Figure 3b illustrates the land use distribution in the inner (d02) domain for the simulations employing the BEP-BEM  
UCM.

180 The land use categories inside the area of interest (Paris region, Île-de-France) are shown in Figure 3c and 3d for BULK and  
BEP-BEM simulations, respectively. Beyond the increased urban detail provided by the BEP-BEM scheme through the use  
of LCZs, it was found that urban grid cells in the BEP-BEM simulations (LCZ classes) cover a larger portion of Île-de-France  
(23.4%) compared to the urban area represented in the BULK simulations (16.6%) (Tables S3 and S4). As noted previously,  
not all land-use classes of the IGBP MODIS classification are present within the area of interest.

185

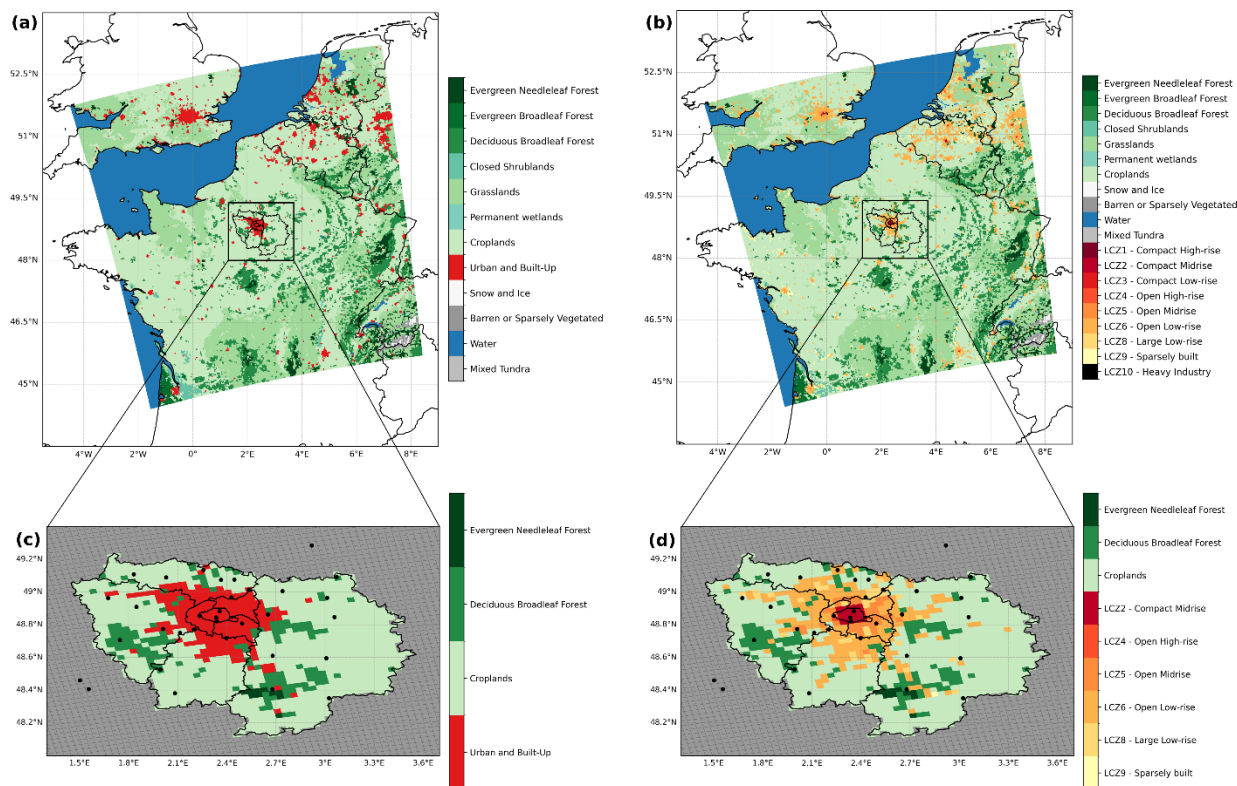


**Figure 3: Land use in the inner domain (d02) and Paris region (Île-de-France) for: BULK run (left column) and BEP-BEM runs (right column).**

## 2.4 WRF simulations

190 In this study, three simulations have been conducted: 1) PAR, in which urban canopy parameters specifically tailored to the Paris region and derived from EO data were applied; 2) CTRL, with the default UCPs used in WRF version 4.6.0; and 3) BULK, in which no UCM is activated. To evaluate the performance of the simulations in the representation of the UHI over the Paris area, two masks (Figure 4) – representing the urban core area and its rural surroundings – were created following the methodology of Diez-Sierra et al. (2025). These masks were based on threshold values of variables inside WRF, such as the urban fraction and additional static inputs such as terrain height and land-use fraction. This procedure effectively excludes the influence of altitude on temperature (i.e., adiabatic lapse rate), enabling a more accurate assessment of the UHI. As an additional refinement to this approach, in the urban mask we included only those urban grid cells (only after fulfilling the abovementioned criteria) located within the GHS-UCDB polygon, providing a more precise delineation of the urban area for mask generation. The magnitude of modelled UHI was then evaluated against the observed from stations located within the two masks. Only urban (non-urban) grid cells were included in the urban (rural) mask, while a buffer zone was considered

195

200

between the two masks to avoid overlap effects (Hawkins et al., 2003).

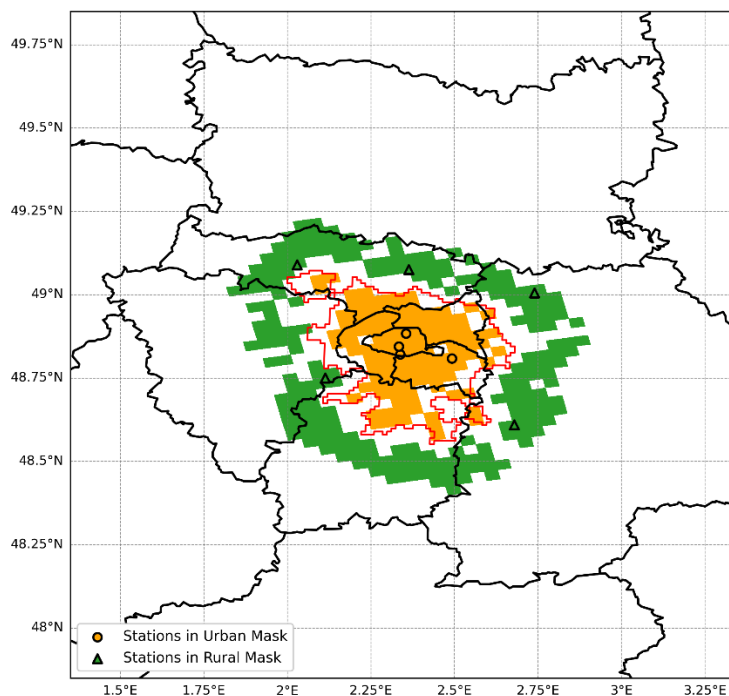


**Figure 4: Urban (orange) and rural mask (green). Dot (triangle) markers correspond to urban (rural) stations inside the urban (rural) mask, while the red polygon represents the urban area of Paris, according to GHS–UCDB polygons.**

## 205 2.5 Observations

Observational data were obtained from the Météo–France RADOME network, which comprises 51 stations around the greater Paris region, and provides measurements at 6–minute intervals. The stations are classified as urban or rural based on the GHS–UCDB polygons. To minimize the impact of data gaps, only stations with less than 1% missing observations relative to the total number of expected records were retained. In addition, to assess consistency between the station classifications and the land–use categories represented in the WRF simulations, a comparison revealed that for 9 stations the land–use category for their nearest model grid cells did not correspond to the actual land use, due to the coarse resolution of the model grid. Consequently, a total of 33 stations were ultimately used to evaluate the WRF simulations, focusing on 2 m air temperature, divided into two groups: “Urban” and “Non–Urban” stations. Of the 33 stations, 13 are associated with model grid cells classified as urban land–use types (“Urban and Built–Up” for BULK, LCZ2, LCZ5, LCZ6 and LCZ8 for BEP–BEM runs).  
215 The remaining 20 stations correspond to grid cells whose land–use categories are either “Croplands” or “Deciduous Broadleaf Forest” across all three simulations. Regarding the UHI evaluation, which was held with the use of the created urban and rural masks, observations only for those stations (nine in total) inside the two masks were utilized (Figure 4).

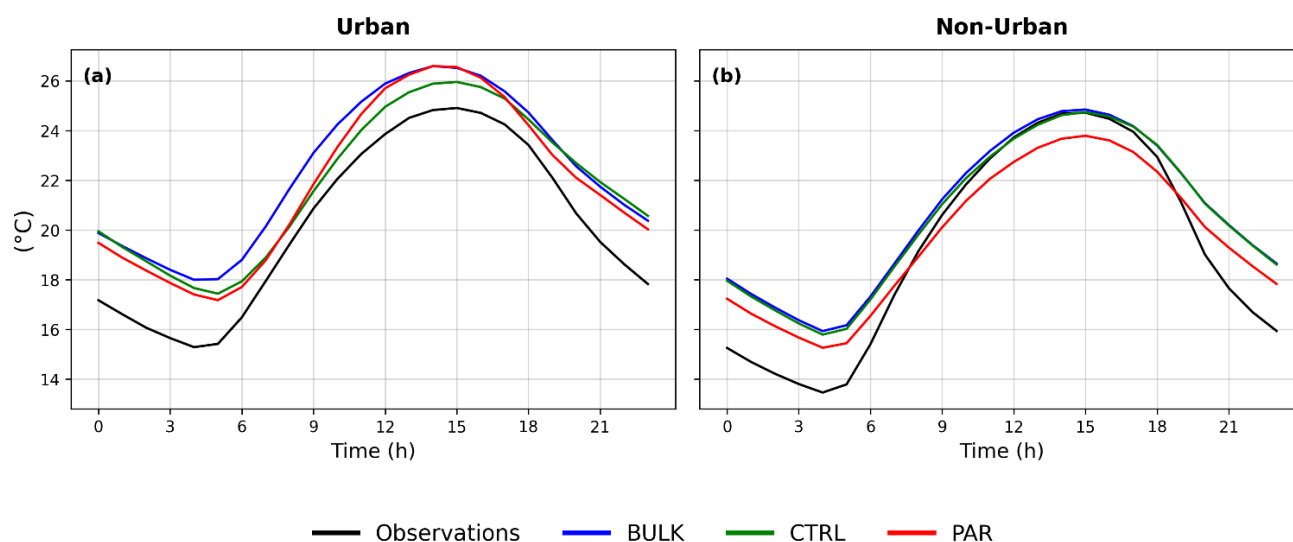


### 3. Results

#### 3.1 Model performance during summer 2020

220 Figure 5 shows the daily cycles for the two groups of stations averaged for the summer months (JJA) of 2020. Over urban stations (Fig. 5a), the 2 m air temperature is overestimated by all three simulations throughout the summer and across the entire diurnal cycle. Month to month variation is shown in the supplementary material (Fig. S1). According to Table 2, the warm bias is systematically larger during nighttime (18:00–07:00 UTC) than during daytime (06:00–17:00 UTC) for all WRF simulations. Activation of the UCM reduces the warm bias compared to BULK, particularly during daytime (1.95 °C in BULK, 1.02 °C in CTRL, 1.53 °C in PAR), but has a negligible impact at night, lowering the bias by just 0.07 °C in CTRL and 0.2 °C in PAR. Therefore, in terms of overall model error (RMSE) the CTRL simulation performs better during daytime, while the PAR configuration performs better during nighttime. The temporal correlation – associated with the 24h diurnal cycle – remains practically the same for the three simulations.

In non-urban areas (Fig. 5b) all simulations perform better during daytime with biases below 0.5 °C, retaining the higher nighttime warm bias (Table 2). Introduction of the PAR configuration alters mostly the model behavior, since it is colder than the other two simulations both during the day and night. This leads to an improvement regarding nighttime hours, since PAR has the smallest bias during the night (1.62°C), alongside with the lowest RMSE values among all three simulations and the highest temporal correlation. However, it also exhibits cold biases during the daytime.



235 **Figure 5: Daily profiles of 2 m air temperature from observations (black), BULK (blue), CTRL (green) and PAR (red) for: (a) Urban; (b) Non-Urban stations, during the summer (JJA) of 2020.**



240

**Table 2: Statistical analysis (Bias, RMSE) of the three simulations concerning group stations (Urban, Non–Urban) during daytime and nighttime hours (indicated as D and N, respectively), for the summer (JJA) of 2020. Temporal correlation (R) is calculated on the totality of the 24h span.**

Simulations	BULK				CTRL				PAR			
	Urban		Non–Urban		Urban		Non–Urban		Urban		Non–Urban	
Group Stations	Urban	Non–Urban	Urban	Non–Urban	Urban	Non–Urban	Urban	Non–Urban	Urban	Non–Urban	Urban	Non–Urban
Day Period	D	N	D	N	D	N	D	N	D	N	D	N
Bias (°C)	1.95	2.36	0.53	2.28	1.02	2.29	0.37	2.21	1.53	2.14	-0.26	1.62
RMSE (°C)	3.59	3.38	3.01	3.51	2.74	3.37	2.62	3.35	3.43	3.49	2.57	3.12
R	0.87		0.86		0.88		0.88		0.86		0.91	

To further investigate the warm bias of WRF over urban areas, we perform a more detailed analysis over distinct LCZs, which correspond to urban land–use for BEP–BEM simulations, namely: LCZ2 (compact high–rise), LCZ5 (open midrise), LCZ6 (open lowrise), LCZ8 (large lowrise). Out of the 13 urban stations in the Météo–France RADOME network, three are classified as LCZ2 (Paris city centre), three as LCZ5, five as LCZ6, and two as LCZ8 (city outskirts). Although the BULK simulation does not use the LCZ land–use classification to urban grid cells (unlike the two BEP–BEM simulations), we extracted BULK values from the corresponding grid cells so that diurnal cycles could be compared across LCZ classes (Fig. 6). This allows the evaluation of whether incorporating the LCZ–driven heterogeneity improves the simulated urban climate. Month to month variation can be obtained in Figure S2.

When the UCM is activated, the highest temperature overestimation occurs over LCZ2 stations (Fig. 6a), which is the most urbanized part of the greater Paris region. The mean biases over the complete 24h diurnal cycle are 1.84 °C and 2.42 °C for the CTRL and PAR simulations, respectively (Table 3). Moving outside the city’s core over LCZ5 stations (Fig. 6b), the magnitude of the warm bias during the 24h span remains relatively the same to that of LCZ2 for CTRL and decreases for the PAR configuration by approximately 0.5 °C (1.86 °C and 1.91 °C, respectively). PAR better performs over stations located at LCZ6 and LCZ8 (Fig. 6c,d) by further reducing the warm biases and slightly outperforming CTRL (Table 3). RMSE values come in accordance with biases, with CTRL (PAR) having the smaller deviations from observational values for LCZ2 and LCZ5 (LCZ6 and LCZ8). Temporal correlations in the diurnal cycles are slightly better for LCZ8 for the two simulations. Furthermore, BULK shows warm biases of similar magnitude across all LCZs, which reflects the limited urban variability captured when urban areas are represented using a single land–use category. The analysis separated into daytime and nighttime period (Table S5) indicate the same pattern found in the urban stations group, with substantially warmer biases during the night than midday for both BEP–BEM simulations across all LCZs.

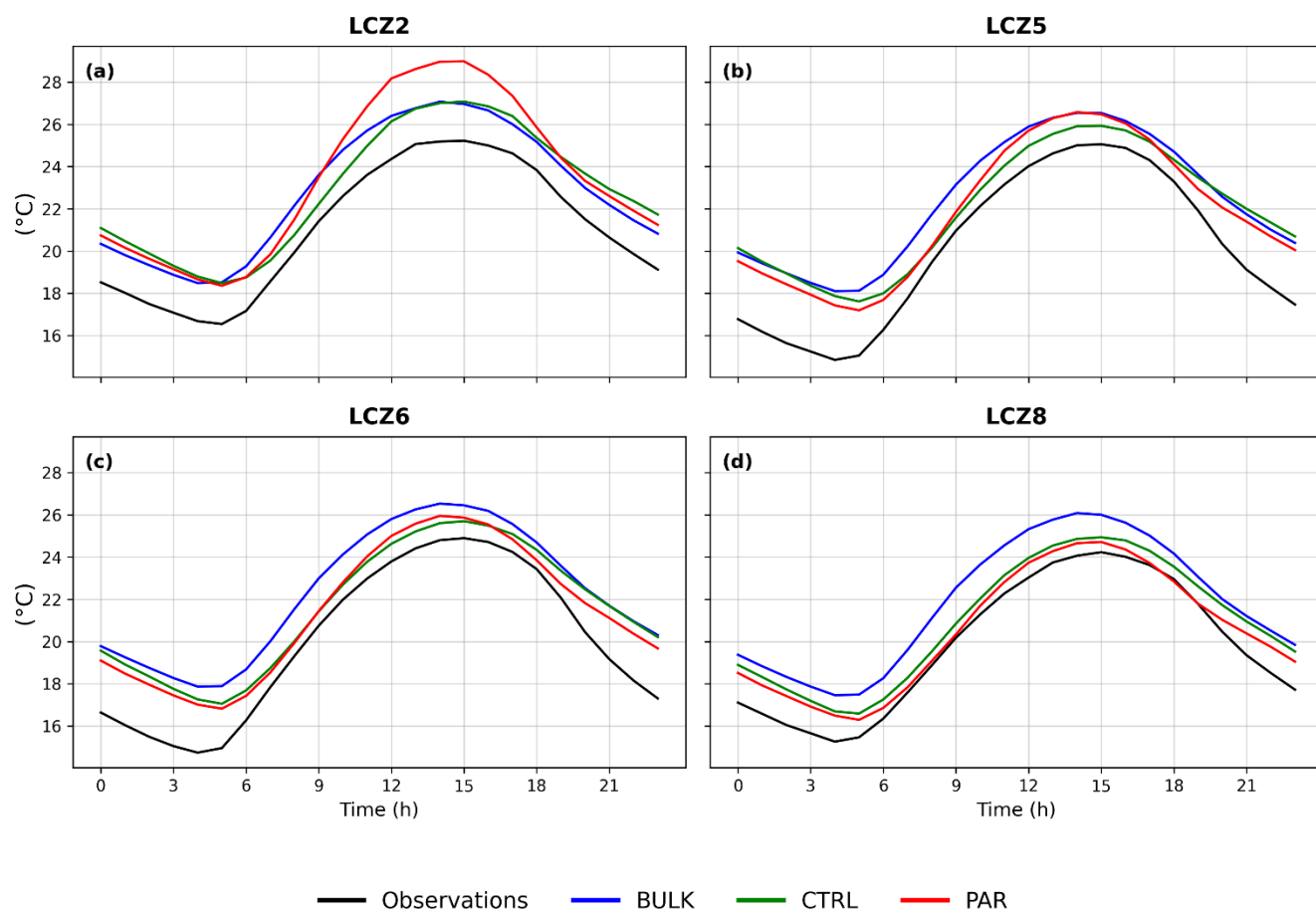


**Figure 6:** Daily profiles of 2 m air temperature from observations (black), BULK (blue), CTRL (green) and PAR (red) for: (a) LCZ2; (b) LCZ5; (c) LCZ6 and (d) LCZ8 stations, during the summer (JJA) of 2020.

265

**Table 3:** Mean diurnal statistical analysis (Bias, RMSE, R) of the two simulations using the BEP–BEM UCM, for stations located at corresponding LCZs, for the summer (JJA) of 2020.

Simulations	CTRL				PAR			
	LCZ2	LCZ5	LCZ6	LCZ8	LCZ2	LCZ5	LCZ6	LCZ8
Group Stations	LCZ2	LCZ5	LCZ6	LCZ8	LCZ2	LCZ5	LCZ6	LCZ8
Bias (°C)	1.84	1.86	1.61	1.10	2.42	1.91	1.45	0.92
RMSE (°C)	3.12	3.39	3.05	2.50	3.53	3.43	2.81	2.11
R	0.88	0.86	0.88	0.90	0.87	0.86	0.88	0.91

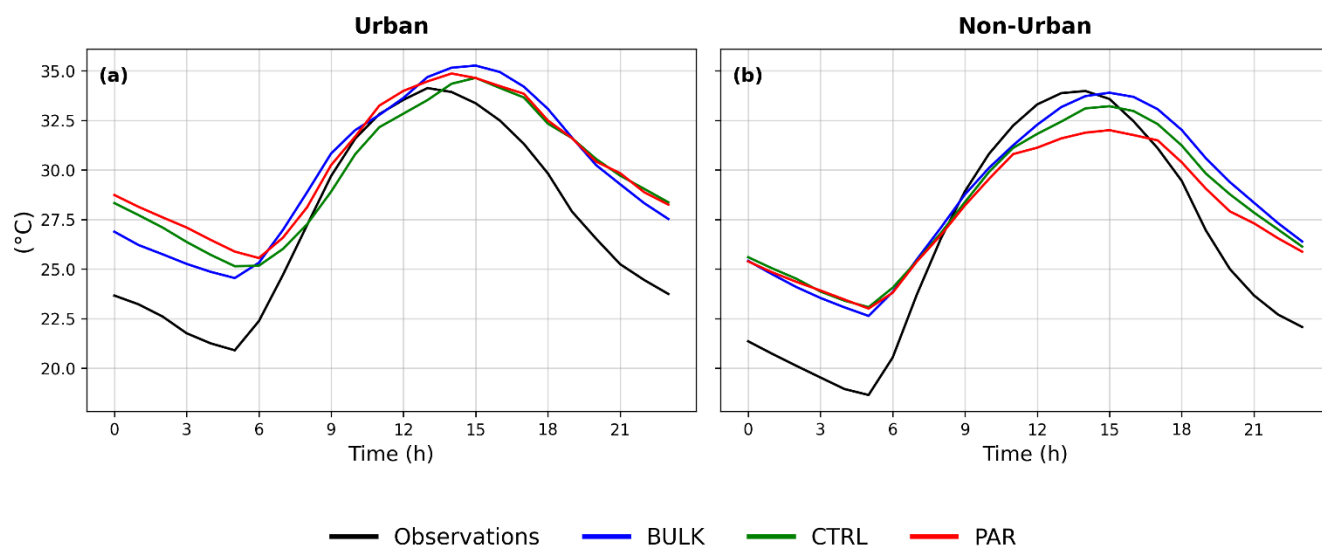


### 3.2 Model performance during the Heatwave of August 2020

270 We investigate the model's performance during a heatwave event occurred from 7 to 13 August 2020 that affected western Europe, including the Paris region, with temperatures reaching up to 40 °C (<https://climate.copernicus.eu/surface-air-temperature-august-2020>). In both station groups (Urban and Non-Urban) the modelled diurnal cycles reveal a one to two-hour lag in the occurrence of maximum temperatures compared to observations (Fig. 7a,b), while this lag is also apparent in the BEP-BEM simulations for minimum temperatures in urban stations. During this heatwave period all three simulations show a warm bias over urban stations, which is consistently higher during nighttime (Fig. 7a). Activation of the UCM alleviates the daytime warm bias (1.45°C in BULK, 0.53°C in CTRL) but deteriorates the nighttime bias (3.52°C in BULK, 4.25°C in CTRL) (Table S6). It seems that urban heat is overproduced in the city centre and there is not sufficient cooling urban mechanisms to allow the city release the excess heat especially during the night.

At Non-Urban stations, again all three simulations exhibit prominent warm biases during the night (Fig. 7b). PAR simulation (Table 4) has the lowest RMSE and the highest time-correlation, slightly outperforming CTRL. BULK has the largest bias, while among the two BEP-BEM simulations, the implementation of EO data (through PAR) improves the model performance compared to CTRL (Table 4), with a decreased bias of 0.17 °C (1.82 °C and 1.99°C, respectively).

Analysis by LCZ (Figure 8 and Table 5) shows this excessive warm bias over the urban cells is concentrated in the most urbanized part of the city (stations for which the nearest grid cell is in LCZ2), which decreases towards the city outskirts. Temperatures are sensitive to the newly introduced PAR configuration, with the largest deviation from the CTRL simulation occurring in LCZ2 stations (warm biases of 3.62 °C and 2.47 °C, respectively). This indicates that the specifics of PAR overestimate the heat generated within the city core. The lower the urbanization of the area, the smaller the warm bias in the 24h span (Table 5) for PAR (3.28 °C, 2.78 °C, 1.65 °C for LCZ5, LCZ6, LCZ8, respectively). The difference between the two BEP-BEM simulations in LCZ2 is larger during sunlight hours and not during the night. The highest warm bias occurs during nighttime across all LCZs (Table S7). This behavior can be explained by the fact that BEP-BEM parameterization is able to store more energy in the urban fabric during the day (Martilli et al., 2002), allowing the formation of a more intense nocturnal urban heat island during the heatwave. Furthermore, the BouLac Planetary Boundary Layer scheme is found to cause nighttime overestimations of temperature in urban related grid cells (Segura et al., 2021), thus also partially explaining the nighttime warm bias not only of BEP-BEM simulations but also that of BULK.

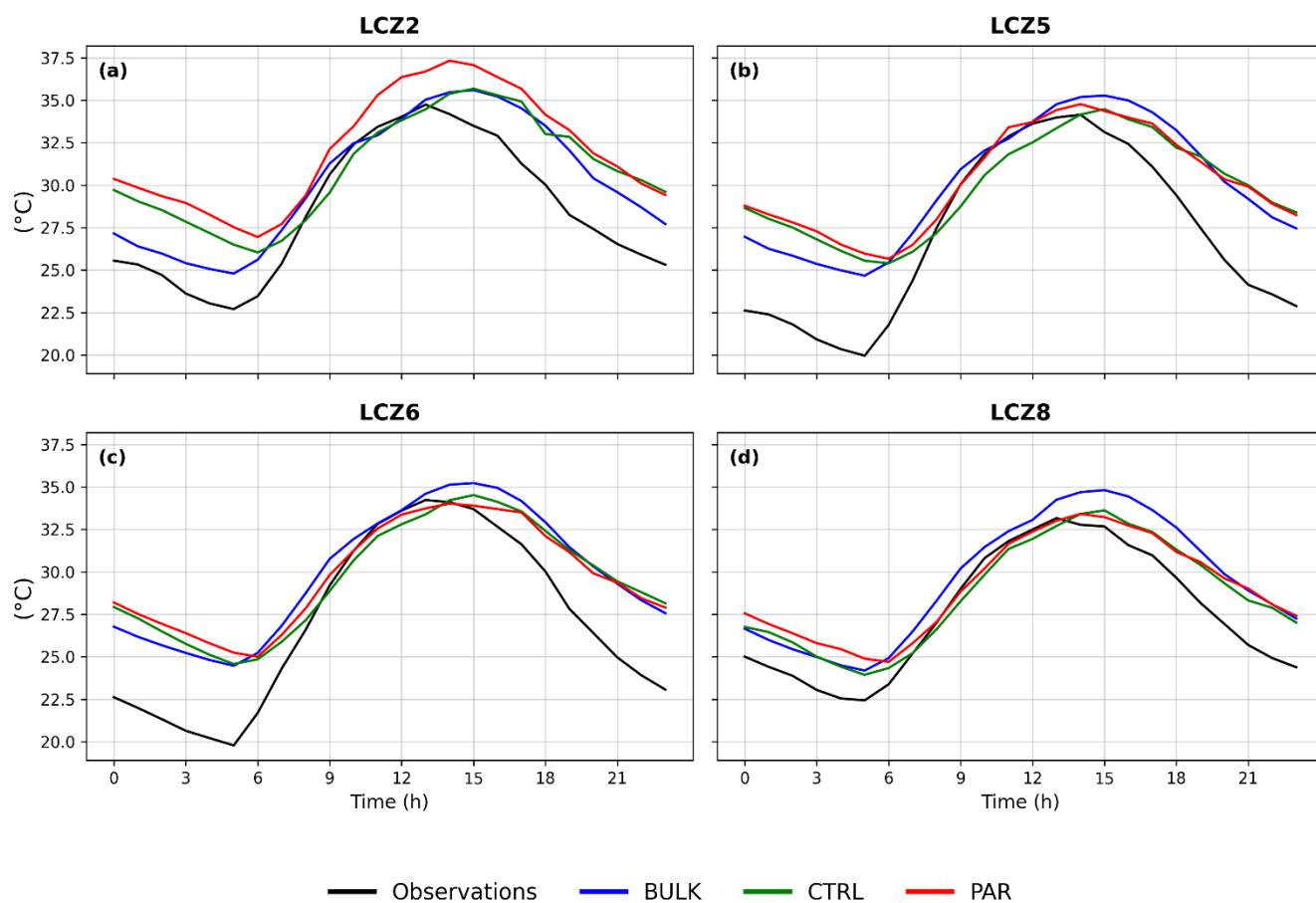


295

**Figure 7: Daily profiles of 2 m temperature from observations (black), BULK (blue), CTRL (green) and PAR (red) for: (a) Urban; (b) Non-Urban stations, during the heatwave event of August 2020.**

**300 Table 4: Mean diurnal statistical analysis (Bias, RMSE, R) of the three simulations, concerning group stations (Urban, Non-Urban), for the heatwave of August 2020.**

Simulations	BULK		CTRL		PAR	
	Urban	Non-Urban	Urban	Non-Urban	Urban	Non-Urban
Bias (°C)	2.48	2.23	2.46	1.99	2.92	1.82
RMSE (°C)	4.41	4.46	4.41	4.00	4.68	3.91
R	0.76	0.79	0.80	0.85	0.78	0.86



— Observations — BULK — CTRL — PAR

305 **Figure 8: Daily profiles of 2 m air temperature from observations (black), BULK (blue), CTRL (green) and PAR (red) for: (a) LCZ2; (b) LCZ5; (c) LCZ6 and (d) LCZ8 stations, during the heatwave of August 2020.**

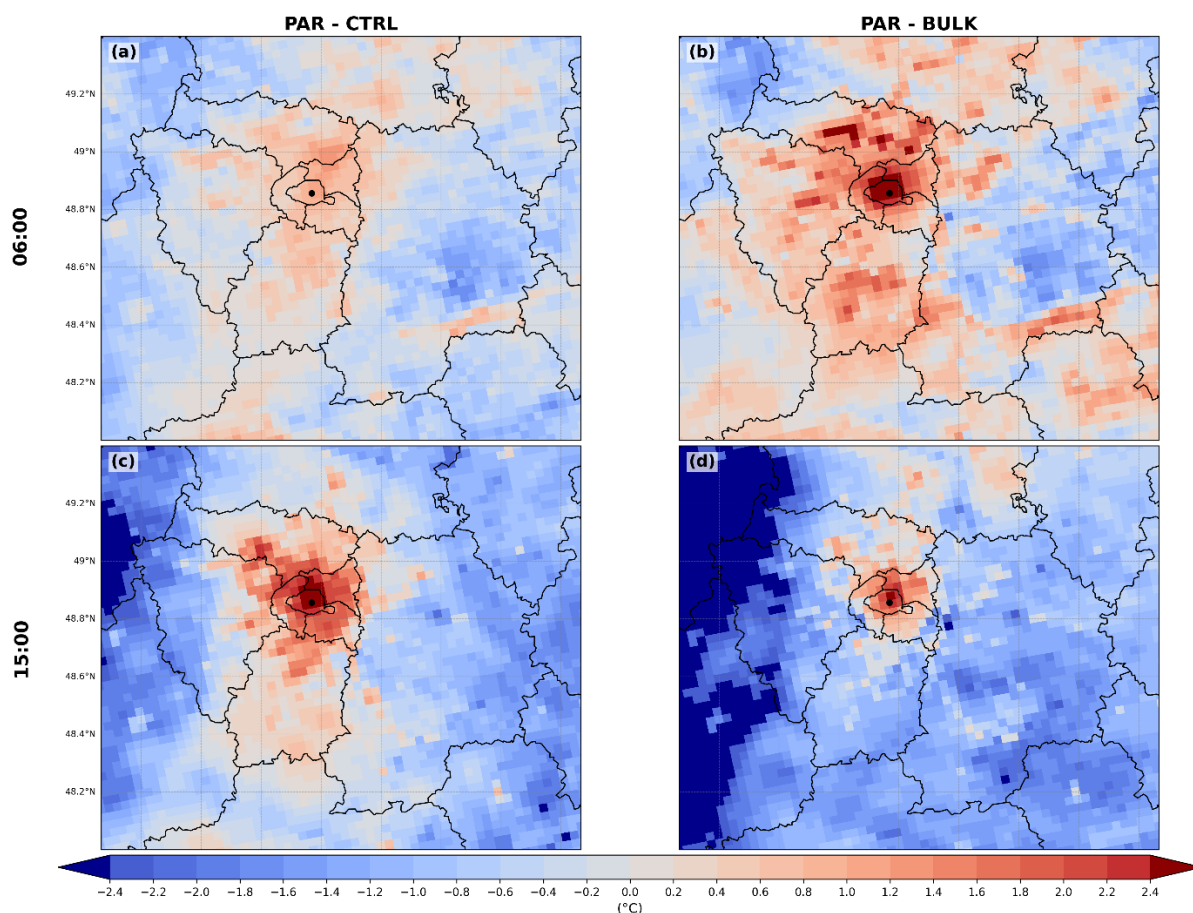
**Table 5: Same as Table 3, but for the heatwave of August 2020.**

Simulations	CTRL				PAR			
	LCZ2	LCZ5	LCZ6	LCZ8	LCZ2	LCZ5	LCZ6	LCZ8
Group Stations	LCZ2	LCZ5	LCZ6	LCZ8	LCZ2	LCZ5	LCZ6	LCZ8
Bias (°C)	2.47	2.87	2.55	1.58	3.62	3.28	2.78	1.65
RMSE (°C)	4.02	4.86	4.18	2.88	4.93	5.16	4.65	3.65
R	0.79	0.76	0.84	0.83	0.76	0.79	0.86	0.81



310 Figure 9 presents the averaged 2 m air temperature differences, when minimum and maximum temperatures occur at approximately 06:00 (upper panel) and 15:00 UTC (bottom panel), respectively, to highlight the spatial differences between the PAR configuration and the other two simulations, CTRL (left panel) and BULK (right panel) during the heatwave. There is not much difference between the PAR and the CTRL simulations for minimum temperatures (Fig. 9a); in contrast, differences between the two simulations are found within the city core at maximum temperatures (Fig. 9c). On the other hand, activation of the UCM (PAR vs BULK) appears to substantially affect minimum temperatures across a large portion of the domain and Paris greater area (Fig. 9b), leading to an increase in minimum temperatures. The colder daytime climatology of PAR at the non-urban areas is also apparent spatially when compared with the CTRL and BULK simulations (Fig. 9c,d). This feature of the PAR simulation may lead to an overestimation in the magnitude of the daytime UHI effect, which is discussed in the following section (3.3).

315



320

**Figure 9: Averaged differences in 2 m air temperature for the heatwave period: (a,c) PAR minus CTRL (left column); (b,d) PAR minus BULK (right column), over 06h (upper panel) and 15h UTC (lower panel).**



### 3.3 Urban Heat Island representation

One of the main objectives of urban parameterizations implemented in numerical regional climate models is to accurately represent the UHI phenomenon, i.e. the temperature contrast between temperature in urban and non-urban areas. The UHI for each simulation is calculated as the difference between urban and rural temperatures, using minimum temperatures for nighttime-UHI and maximum temperatures for daytime-UHI. In both cases, the mean temperature of the grid cells within the rural mask (207 in total) is used as a reference, and temperature anomalies for all grid cells – both urban and rural – are computed relative to this value. In this way, the anomalies within the rural mask average to zero, while those within the urban mask average to the mean urban heat island intensity (UHII). The urban mask contains 109 grid cells. Figure 10 shows the daily nocturnal (left) and diurnal (right) UHII for August 2020 for BULK (top), CTRL (middle) and PAR (bottom). The pink shaded areas represent the values for all grid cells of the urban mask, indicating the range of UHII variability. The average UHII is also indicated in the plot (thick red line). The green shaded areas indicate values for all grid cells of the rural mask, averaging to zero (thick green line). We also calculate the observed UHII comparing the mean temperature of the stations lying within the urban mask to that of the stations in the rural mask (black dashed line). The mean observed rural temperature, albeit different from the mean model rural temperature, is also depicted in Fig. 10 as a line with zero value parallel to the x-axis, since it serves as a reference to the observed UHII.

The nocturnal UHII in CTRL is strong, like the observed. This can be interpreted as a confirmation of the correctness of the UCM physical process, according to which during night rural areas cool faster than urban areas, while urban areas store large amounts of heat and release it slowly at night. The BULK simulation produces a relatively flat UHII range of approximately 2–3 °C, whereas observations show substantially greater day-to-day variability, ranging from 1 to 5 °C. PAR reproduces even better the variability and strength of the observed nocturnal UHII, indicating that the tailored parameters for urban environment can moderate significantly nighttime temperatures. The diurnal UHII is moderate (1-2 °C) according to observations and appropriately reproduced by the BEP-BEM simulation. With the PAR configuration the diurnal UHII becomes unrealistically strong (2-4 °C), indicating that the urban environment heats up a lot during the day, eventually as a result of the EO-derived urban morphological characteristics and their source-area selection, which is discussed in the following section. This lead to taller buildings and narrower streets compared to default values inside the WRF lookup table, which potentially enhanced heat retention.

It should furthermore be emphasized that the agreement between modelled and observed UHII on certain days does not necessarily indicate an accurate simulation of the underlying temperature fields. For instance, during the heatwave event, the simulations exhibit a pronounced overestimation of nighttime 2 m air temperature. As a result, the modeled UHII may reproduce the observed intensity while being based on temperatures that are systematically higher than the observed. Nevertheless, urban and rural masks consistently capture the urban-rural temperature contrast, which demonstrates that the masks for grid cell selection are a well suited tool.



355

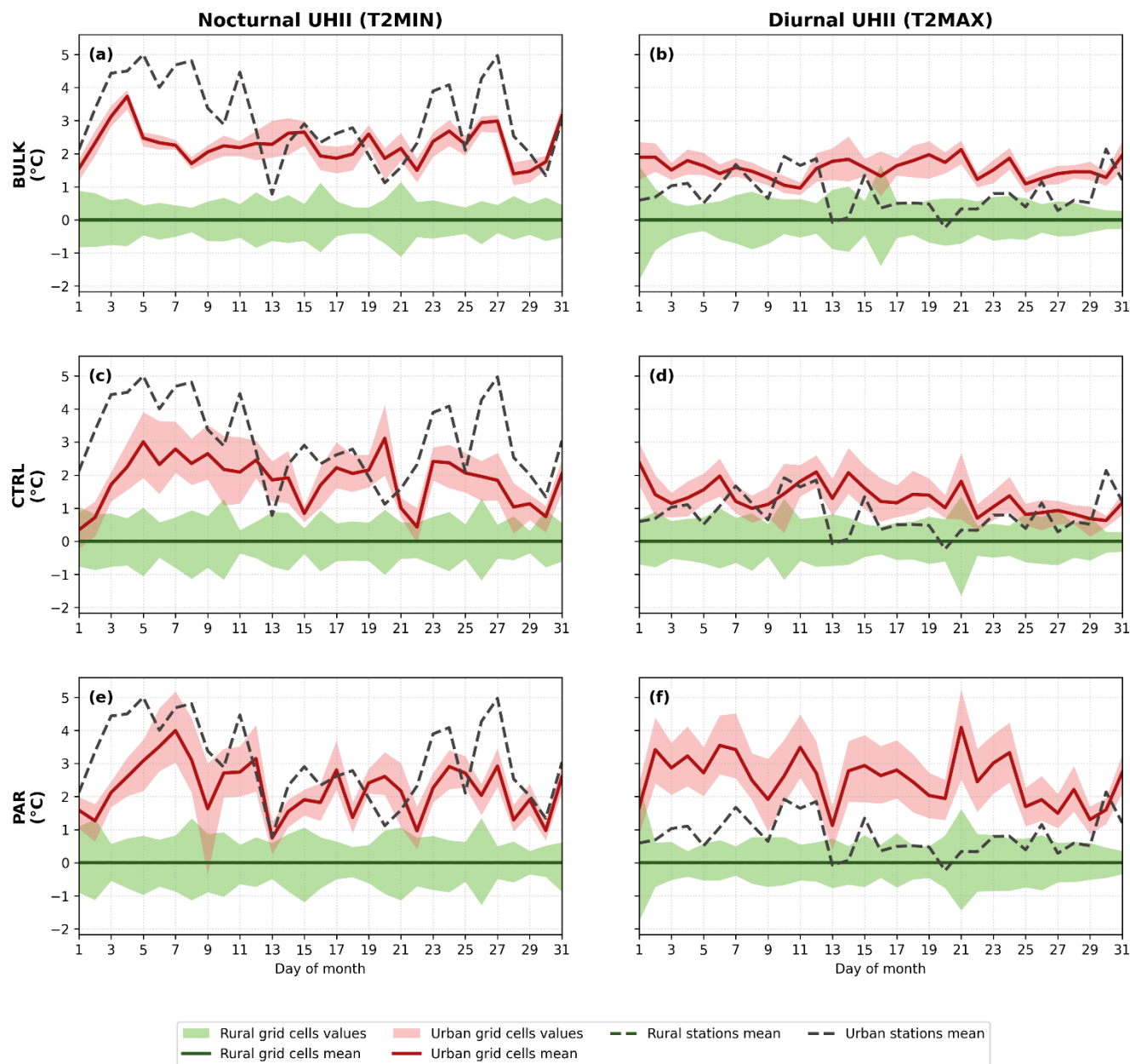


**Figure 10: Nocturnal (left column) and diurnal (right column) UHII for August 2020, seen by BULK (a,b); CTRL (c,d) and PAR (e,f). Black dashed line indicates the observed urban heat island from the stations located within the two masks.**



#### 4. Summary and Conclusions

360 The present study investigates the impact of the BEP–BEM UCM implemented within WRF on temperatures and UHI  
representation of the greater Paris area. We performed three simulations: a) BULK, which is the most simplistic approach of  
the urban environment representation within WRF, as no UCM is switched on and the urban areas are represented as one land  
use category b) CTRL, in which the most complex multilayer UCM is switched on with the default WRF urban canopy  
parameters (as of version 4.6.0) and urban areas are represented by the urban LCZ classes and c) PAR, which used the same  
365 setting as CTRL, but with Paris–tailored urban canopy parameters, based on high–resolution EO data. The analysis covers the  
time period from June to August 2020 and is compared to available observations from the RADOME network.

Over urban areas, the BULK configuration shows a persistent warm bias. During the whole summer period, the warm bias is  
mitigated when the BEP–BEM UCM is activated. The JJA daytime bias for the BULK simulation is 1.95 °C and it is reduced  
to 1.02 °C in CTRL. The PAR configuration produces more urban heat than CTRL, adding to the overall CTRL warm daytime  
370 bias (1.53 °C). Nighttime warm biases are consistently higher than daytime biases in BULK and are slightly decreased with  
the coupled BEP–BEM UCM (decreased by 0.07 °C for CTRL) and further decreased by 0.22 °C for the PAR configuration.  
To better assess how the degree of urbanization introduced in the model affects temperature, we conduct an LCZ–based  
analysis. In both BEP–BEM simulations a warmer environment is produced at the most urbanized zones (LCZ2 and LCZ5).  
During the heatwave event of August 2020 in Paris the warm biases become more severe. Implementation of the Paris–tailored  
375 UCPs in WRF results in even higher warm biases over all LCZs.

At the non–urban areas, the PAR configuration has the most distinct performance compared to the other two simulations, and  
achieves the best overall performance with the lowest RMSE both in day and night, during the summer months. It also keeps  
daytime bias lower (–0.26°C), reduces the nighttime bias to 1.62°C and the temporal correlation is the highest (0.91). When  
the heatwave of August 2020 is investigated, the same results hold true: RMSE, bias and temporal correlation are best for the  
380 PAR simulation over the non–urban areas.

Investigation of the UHII provides information about the temperature contrasts between the urban and non–urban areas. In  
general, the nocturnal UHI as a phenomenon is stronger than the daytime UHI, because during nighttime urban regions release  
the heat stored during the day, anthropogenic heat may be additionally added, while rural areas cool faster, thus amplifying  
the temperature contrast between urban vs rural areas. Indeed, the nocturnal UHII in CTRL is strong and similar to the observed  
385 (RADOME). This can be interpreted as a confirmation of the correct representation of the physical process within the urban  
canopy, according to which during night rural areas cool faster than urban areas, while urban areas store large amounts of heat  
and release it slowly at night. PAR reproduces the strong nocturnal UHII better, indicating an improved representation of the  
contrast between urban and non–urban nighttime environments. The diurnal UHII is moderate according to observations (1–2  
°C) and appropriately reproduced by the CTRL simulation. For the PAR configuration, the diurnal UHII becomes



390 unrealistically strong (2-4 °C), indicating that there is too much heat trapped in the urbanized zones of the city, while non-urban regions remain cooler during daytime. The BULK configuration underestimates the UHI effect, as it poorly discriminates urban vs rural environments.

Our overall conclusion on the behavior of the coupled BEP-BEM UCM is that it improves model performance. The additional configuration with UCPs tailored for Paris region (PAR) improves specific aspects of the model performance (like nighttime  
395 temperatures over non-urban areas), without being consistently better than the CTRL configuration, or systematically worse. Both BEP-BEM configurations replicate in a more accurate and realistic way the urban temperature spatial patterns in comparison to the BULK simulation, which represents the city as a homogenous space. The performance of the PAR simulation depends very much on the way that EO data has been implemented into the WRF model. As a result, while the PAR configuration had the more detailed representation for Paris region, the UCPs tailored for this area are based only from a  
400 fraction of the wider area of Paris city, specifically from the core of the city (see Fig. 2). This potentially led to misrepresentations of parameters such as albedo and emissivity as long as the morphological ones, whose values are expected to be altered in the vicinity of the city center, but were universally applied to the whole area. For instance, inside the area from where the UCPs for PAR simulation are tailored, LCZ2 urban grid cells do not extend beyond, but LCZ5, LCZ6 and LCZ8 can be found also in a wider area from the one mentioned. Thus, the three latter LCZs obtained values that were representative  
405 to the department of Paris and its three adjacent departments, potentially “widening” the city’s center core characteristics further beyond and leading to such overestimations. Additionally, because LCZ6 and LCZ8 have the biggest coverage of all LCZs in Paris region (see Tables S3 and S4), plus that PAR exhibits higher buildings in these classes than CTRL (see Figure S3), an exaggeration of heat accumulation in Paris’ center core may take place in PAR simulation compared to CTRL. Indeed, the LCZ-based evaluation analysis indicates that the warmest biases appear in the most urbanized zone (compact high-rise)  
410 and are close to zero to the less urbanized environment (large lowrise).

The main recommendations arising from this study can be summarized as follows:

- 1) Activation of the UCM in WRF is highly recommended for numerical studies, particularly if the added computational cost (~ +25% compared to BULK simulation) can be afforded. The official CMIP6/EURO-CORDEX WRF configuration (WRF451Q in the Balanced Ensemble Design) (Sobolowski et al., 2025) is based on the urban option  
415 BULK, which captures some aspects of the urban climate (Langendijk et al., 2025); however, its representation remains less accurate than more advanced urban schemes.
- 2) Improved representation of urban, green, and blue spaces using urban EO data from European datasets (e.g., Copernicus) is expected to significantly enhance city-scale simulations, contingent upon parallel advancements in UCM capabilities. The EO-based city tailored information should cover the wider city area (not just the city core) to  
420 address properly all distinct urban characteristics. Ideally, the creation of a gridded dataset applicable in WRF in



convection-permitting resolutions, with the morphological characteristics not only for the area of interest, but for every city in the globe, would lead to a more accurate urban representation of the whole domain.

The results of this study have some limitations. In particular, the analysis period (JJA 2020) is relatively short for climate-scale assessments. Despite this limitation, the consistency of the results supports their reliability for assessing the usefulness of BEP-BEM and its configuration within WRF. The impact of urban anthropogenic heat was not explicitly investigated in this study. Following the WRF default configuration, anthropogenic urban heat emissions were assumed to be constant over 24 hours, an assumption that likely overestimates actual conditions. This simplification may contribute to the overproduction of urban heat in the present simulations. Future studies should revisit this assumption by incorporating more realistic diurnal profiles of anthropogenic heat emissions, ideally derived from national statistics on air-conditioning usage.

#### 430 **Code and data availability**

The run folder of WRF v4.5.1 model with the modified UCP lookup table (under the name URBPARAM\_LCZ\_Paris.TBL) and the observational data from the Météo-France RADOME network used for validation are available at <https://doi.org/10.5281/zenodo.19253784> (Kyriakidis et al., 2026).

#### **Author contributions**

435 This study was conceptualized by EK and VP. The methodology was made by IK, VP, JM, EK, while software, analysis and validation was conducted by IK and MG. VP, IK and ZM took part in the research investigation, while EK, VP, JF and NC supervised the study. Visualisation was made by IK. VP and IK ran the model, while IK wrote the paper with contributions from all authors.

#### **Competing interests**

440 The contact author has declared that none of the authors has any competing interests.

#### **Acknowledgements**

The authors would like to acknowledge the CORDEX-Flagship Pilot Study on “Urban environment and Regional Climate Change” (URB-RCC) for providing the framework of the regional urban climate simulations. We also acknowledge Météo-France for providing the standard meteorological variables used in this study, and the French national center for Atmospheric data and services AERIS for granting access to the data. This work was supported by computational time granted from the 445 National Infrastructures for Research and Technology S.A. (GRNET S.A.) in the National HPC facility - ARIS - under project



ID pr017036\_thin - “FPS–urban Testing phase”. Results presented in this work have been also produced using the AUTH Compute Infrastructure and Resources. JM acknowledges funding by the Ministry for the Ecological Transition and the Demographic Challenge (MITECO) and the European Commission NextGenerationEU (Regulation EU 2020/2094), through  
450 CSIC's Interdisciplinary Thematic Platform Clima (PTI-Clima).

### Financial support

This study is part of the research project UpClim, which was implemented in the framework of H.F.R.I. called “Basic Research Financing (Horizontal Support of All Sciences)” under the National Recovery and Resilience Plan “Greece 2.0”, funded by the European Union–NextGenerationEU (H.F.R.I. Project Number: 14696).

### 455 References

- Bougeault, P. and Lacarrere, P.: Parameterization of Orography-Induced Turbulence in a Mesobeta--Scale Model, [https://doi.org/https://doi.org/10.1175/1520-0493\(1989\)117%3C1872:POOITI%3E2.0.CO;2](https://doi.org/https://doi.org/10.1175/1520-0493(1989)117%3C1872:POOITI%3E2.0.CO;2), 1989.
- Britter, R. E. and Hanna, S. R.: Flow and dispersion in urban areas, *Annu. Rev. Fluid Mech.*, 35, 469–496, <https://doi.org/10.1146/annurev.fluid.35.101101.161147>, 2003.
- 460 Brousse, O., Martilli, A., Foley, M., Mills, G., and Bechtel, B.: WUDAPT, an efficient land use producing data tool for mesoscale models? Integration of urban LCZ in WRF over Madrid, *Urban Clim.*, 17, 116–134, <https://doi.org/10.1016/j.uclim.2016.04.001>, 2016.
- Chen, F., Kusaka, H., Bornstein, R., Ching, J., Grimmond, C. S. B., Grossman-Clarke, S., Loridan, T., Manning, K. W., Martilli, A., Miao, S., Sailor, D., Salamanca, F. P., Taha, H., Tewari, M., Wang, X., Wyszogrodzki, A. A., and Zhang, C.: The  
465 integrated WRF/urban modelling system: Development, evaluation, and applications to urban environmental problems, *International Journal of Climatology*, 31, 273–288, <https://doi.org/10.1002/joc.2158>, 2011.
- Ching, J., Mills, G., Bechtel, B., See, L., Feddema, J., Wang, X., Ren, C., Brorousse, O., Martilli, A., Neophytou, M., Mouzourides, P., Stewart, I., Hanna, A., Ng, E., Foley, M., Alexander, P., Aliaga, D., Niyogi, D., Shreevastava, A., Bhalachandran, P., Masson, V., Hidalgo, J., Fung, J., Andrade, M., Baklanov, A., Dai, W., Milcinski, G., Demuzere, M.,  
470 Brunsell, N., Pesaresi, M., Miao, S., Mu, Q., Chen, F., and Theeuwesits, N.: WUDAPT: An urban weather, climate, and environmental modeling infrastructure for the anthropocene, *Bull. Am. Meteorol. Soc.*, 99, 1907–1924, <https://doi.org/10.1175/BAMS-D-16-0236.1>, 2018.
- Demuzere, M., Kittner, J., Martilli, A., Mills, G., Moede, C., Stewart, I. D., Van Vliet, J., and Bechtel, B.: A global map of local climate zones to support earth system modelling and urban-scale environmental science, *Earth Syst. Sci. Data*, 14, 3835–  
475 3873, <https://doi.org/10.5194/essd-14-3835-2022>, 2022.



- Diez-Sierra, J., Quintana, Y., Langendijk, G. S., Milovac, J., Demuzere, M., Nogherotto, R., Pietikäinen, J.-P., Rechid, D., Zazulie, N., Solman, S. A., and Fernández, J.: Delineating CORDEX model urban areas and their rural surroundings for megacities worldwide to assess urban climate change, 2025.
- 480 Florczyk, A. J., Melchiorri, M., Corbane, C., Schiavina, M., Maffeni, M., Pesaresi, M., Politis, P., Sabo, S., Freire, S., Ehrlich, D., Kemper, T., Tommasi, P., Airaghi, D., and Zanchetta, L.: Description of the GHS Urban Centre Database, <https://doi.org/10.2760/037310>, 2015.
- Hawkins, T. W., Brazel, A. J., Stefanov, W. L., Bigler, W., and Saffell, E. M.: The Role of Rural Variability in Urban Heat Island Determination for Phoenix, Arizona, [https://doi.org/10.1175/1520-0450\(2004\)043%3C0476:TRORVI%3E2.0.CO;2](https://doi.org/10.1175/1520-0450(2004)043%3C0476:TRORVI%3E2.0.CO;2), 2003.
- 485 Hersbach, H., Bell, B., Berrisford, P., Hirahara, S., Horányi, A., Muñoz-Sabater, J., Nicolas, J., Peubey, C., Radu, R., Schepers, D., Simmons, A., Soci, C., Abdalla, S., Abellan, X., Balsamo, G., Bechtold, P., Biavati, G., Bidlot, J., Bonavita, M., De Chiara, G., Dahlgren, P., Dee, D., Diamantakis, M., Dragani, R., Flemming, J., Forbes, R., Fuentes, M., Geer, A., Haimberger, L., Healy, S., Hogan, R. J., Hólm, E., Janisková, M., Keeley, S., Laloyaux, P., Lopez, P., Lupu, C., Radnoti, G., de Rosnay, P., Rozum, I., Vamborg, F., Villaume, S., and Thépaut, J. N.: The ERA5 global reanalysis, *Quarterly Journal of the Royal Meteorological Society*, 146, 1999–2049, <https://doi.org/10.1002/qj.3803>, 2020.
- 490 Hong, S. Y. and Jang, J.: Impacts of Shallow Convection Processes on a Simulated Boreal Summer Climatology in a Global Atmospheric Model, *Asia. Pac. J. Atmos. Sci.*, 54, 361–370, <https://doi.org/10.1007/s13143-018-0013-3>, 2018.
- Iacono, M. J., Delamere, J. S., Mlawer, E. J., Shephard, M. W., Clough, S. A., and Collins, W. D.: Radiative forcing by long-lived greenhouse gases: Calculations with the AER radiative transfer models, *Journal of Geophysical Research Atmospheres*, 113, <https://doi.org/10.1029/2008JD009944>, 2008.
- 495 Jacob, D., Teichmann, C., Sobolowski, S., Katragkou, E., Anders, I., Belda, M., Benestad, R., Boberg, F., Buonomo, E., Cardoso, R. M., Casanueva, A., Christensen, O. B., Christensen, J. H., Coppola, E., De Cruz, L., Davin, E. L., Dobler, A., Domínguez, M., Fealy, R., Fernandez, J., Gaertner, M. A., García-Díez, M., Giorgi, F., Gobiet, A., Goergen, K., Gómez-Navarro, J. J., Alemán, J. J. G., Gutiérrez, C., Gutiérrez, J. M., Güttler, I., Haensler, A., Halenka, T., Jerez, S., Jiménez-Guerrero, P., Jones, R. G., Keuler, K., Kjellström, E., Knist, S., Kotlarski, S., Maraun, D., van Meijgaard, E., Mercogliano, P., Montávez, J. P., Navarra, A., Nikulin, G., de Noblet-Ducoudré, N., Panitz, H. J., Pfeifer, S., Piazza, M., Pichelli, E., Pietikäinen, J. P., Prein, A. F., Preuschmann, S., Rechid, D., Rockel, B., Romera, R., Sánchez, E., Sieck, K., Soares, P. M. M., Somot, S., Srnec, L., Sørland, S. L., Termonia, P., Truhetz, H., Vautard, R., Warrach-Sagi, K., and Wulfmeyer, V.: Regional climate downscaling over Europe: perspectives from the EURO-CORDEX community, *Reg. Environ. Change*, 20, <https://doi.org/10.1007/s10113-020-01606-9>, 2020.
- 500 Kain, J.: The Kain–Fritsch Convective Parameterization: An Update, *Journal of Applied Meteorology*, 43, 170–181, [https://doi.org/10.1175/1520-0450\(2004\)043<0170:TKCPAU>2.0.CO;2](https://doi.org/10.1175/1520-0450(2004)043<0170:TKCPAU>2.0.CO;2), 2004.
- 505



- Katragkou, E., Sobolowski, S. P., Teichmann, C., Solmon, F., Pavlidis, V., Rechid, D., Hoffmann, P., Fernandez, J., Nikulin, G., and Jacob, D.: Delivering an Improved Framework for the New Generation of CMIP6-Driven EURO-CORDEX Regional Climate Simulations, *Bull. Am. Meteorol. Soc.*, 105, E962–E974, <https://doi.org/10.1175/BAMS-D-23-0131.1>, 2024.
- 510 Kusaka, H. and Kimura, F.: Coupling a Single-Layer Urban Canopy Model with a Simple Atmospheric Model: Impact on Urban Heat Island Simulation for an Idealized Case, *Journal of the Meteorological Society of Japan. Ser. II*, 82, 67–80, <https://doi.org/10.2151/jmsj.82.67>, 2004.
- Kusaka, H., Kondo, H., Kikegawa, Y., and Kimura, F.: A Simple Single-Layer Urban Canopy Model For Atmospheric Models: Comparison With Multi-Layer And Slab Models, *Boundary. Layer. Meteorol.*, 101, 329–358, <https://doi.org/10.1023/A:1019207923078>, 2001.
- 515 Kyriakidis, I., PAVLIDIS, V., Gkolemi, M., Mitraka, Z., Chrysoulakis, N., Milovac, J., Fernández, J., and Katragkou, E.: A new Earth Observation–based WRF configuration for urban regional climate simulations over Paris [Data set]. *Zenodo*. <https://doi.org/10.5281/zenodo.19253784>, 2026.
- 520 Langendijk, G. S., Halenka, T., Hoffmann, P., Adinolfi, M., Aldama Campino, A., Asselin, O., Bastin, S., Bechtel, B., Belda, M., Bushenkova, A., Campanale, A., Chun, K. P., Constantinidou, K., Coppola, E., Demuzere, M., Doan, Q. Van, Evans, J., Feldmann, H., Fernandez, J., Fita, L., Hadjinicolaou, P., Hamdi, R., Hundhausen, M., Grawe, D., Johannsen, F., Milovac, J., Katragkou, E., Kerroumi, N. E. I., Kotlarski, S., Le Roy, B., Lemonsu, A., Lennard, C., Lipson, M., Mandal, S., Muñoz Pabón, L. E., Pavlidis, V., Pietikäinen, J. P., Raffa, M., Raluy-López, E., Rechid, D., Rui, I., Schulz, J. P., Soares, P. M. M., Takane, Y., Teichmann, C., Thatcher, M., Top, S., Van Schaeybroeck, B., Wang, F., and Yuan, J.: Towards better understanding the urban environment and its interactions with regional climate change - The WCRP CORDEX Flagship Pilot Study URB-RCC, *Urban Clim.*, 58, <https://doi.org/10.1016/j.uclim.2024.102165>, 2024.
- 525 Langendijk, G. S., Fernandez, J., Demuzere, M., Diez-Sierra, J., Quintana, Y., Fita, L., Zazulie, N., Nogherotto, R., Carril, A. F., Chun, K. P., Giuliani, G., Halenka, T., Hoffmann, P., Muñoz, L. E., Pietikäinen, J.-P., Rechid, D., and Yuan, J.: Representation of global mega-cities and their urban heat island in CORDEX-CORE regional climate model simulations, *npj Urban Sustainability*, <https://doi.org/10.1038/s42949-025-00325-6>, 2025.
- 530 Liu, Y., Chen, F., Warner, T., and Basara, J.: Verification of a Mesoscale Data-Assimilation and Forecasting System for the Oklahoma City Area during the Joint Urban 2003 Field Project, *J. Appl. Meteorol. Climatol.*, 45, 912–929, <https://doi.org/10.1175/JAM2383.1>, 2006.
- 535 Martilli, A., Clappier, A., and Rotach, M. W.: An Urban Surface Exchange Parameterisation for Mesoscale Models, *Boundary. Layer. Meteorol.*, 104, 261–304, <https://doi.org/10.1023/A:1016099921195>, 2002.
- Martilli, A., Brousse, O., and Ching, J.: Urbanized WRF modeling using WUDAPT, <https://doi.org/10.13140/RG.2.1.3405.2724>, 2016.
- 540 Niu, G. Y., Yang, Z. L., Mitchell, K. E., Chen, F., Ek, M. B., Barlage, M., Kumar, A., Manning, K., Niyogi, D., Rosero, E., Tewari, M., and Xia, Y.: The community Noah land surface model with multiparameterization options (Noah-MP): 1. Model



- description and evaluation with local-scale measurements, *Journal of Geophysical Research Atmospheres*, 116, <https://doi.org/10.1029/2010JD015139>, 2011.
- Reinhart, V., Hoffmann, P., Rechid, D., Böhner, J., and Bechtel, B.: High-resolution land use and land cover dataset for regional climate modelling: a plant functional type map for Europe 2015, *Earth Syst. Sci. Data*, 14, 1735–1794, <https://doi.org/10.5194/essd-14-1735-2022>, 2022.
- 545 Salamanca, F. and Martilli, A.: A new Building Energy Model coupled with an Urban Canopy Parameterization for urban climate simulations-part II. Validation with one dimension off-line simulations, *Theor. Appl. Climatol.*, 99, 345–356, <https://doi.org/10.1007/s00704-009-0143-8>, 2010.
- Salamanca, F., Krpo, A., Martilli, A., and Clappier, A.: A new building energy model coupled with an urban canopy parameterization for urban climate simulations-part I. formulation, verification, and sensitivity analysis of the model, *Theor. Appl. Climatol.*, 99, 331–344, <https://doi.org/10.1007/s00704-009-0142-9>, 2010.
- 550 Segura, R., Badia, A., Ventura, S., Gilabert, J., Martilli, A., and Villalba, G.: Sensitivity study of PBL schemes and soil initialization using the WRF-BEP-BEM model over a Mediterranean coastal city, *Urban Clim.*, 39, <https://doi.org/10.1016/j.uclim.2021.100982>, 2021.
- 555 Skamarock, W. C., Klemp, J. B., Dudhia, J., Gill, D. O., Liu, Z., Berner, J., Wang, W., Powers, J. G., Duda, M. G., Barker, D. M., and Huang, X.-Y.: A Description of the Advanced Research WRF Model Version 4, Boulder, CO, USA, 2021.
- Sobolowski, S., Somot, S., Fernandez, J., Evin, G., Brands, S., Maraun, D., Kotlarski, S., Jury, M., Benestad, R. E., Teichmann, C., Christensen, O. B., Bülow, K., Buonomo, E., Katragkou, E., Steger, C., Sørland, S., Nikulin, G., McSweeney, C., Dobler, A., Palmer, T., Wilcke, R., Boé, J., Brunner, L., Ribes, A., Qasmi, S., Nabat, P., Sevault, F., and Oudar, T.: GCM Selection and Ensemble Design: Best Practices and Recommendations from the EURO-CORDEX Community, *Bull. Am. Meteorol. Soc.*, 106, E1834–E1850, <https://doi.org/10.1175/BAMS-D-23-0189.1>, 2025.
- 560 Stewart, I. D. and Oke, T. R.: Local climate zones for urban temperature studies, *Bull. Am. Meteorol. Soc.*, 93, 1879–1900, <https://doi.org/10.1175/BAMS-D-11-00019.1>, 2012.
- Thompson, G., Rasmussen, R. M., and Manning, K.: Explicit Forecasts of Winter Precipitation Using an Improved Bulk Microphysics Scheme. Part I: Description and Sensitivity Analysis, [https://doi.org/https://doi.org/10.1175/1520-0493\(2004\)132%3C0519:EFOWPU%3E2.0.CO;2](https://doi.org/https://doi.org/10.1175/1520-0493(2004)132%3C0519:EFOWPU%3E2.0.CO;2), 2004.
- 565 Thompson, G., Field, P. R., Rasmussen, R. M., and Hall, W. D.: Explicit forecasts of winter precipitation using an improved bulk microphysics scheme. Part II: Implementation of a new snow parameterization, *Mon. Weather Rev.*, 136, 5095–5115, <https://doi.org/10.1175/2008MWR2387.1>, 2008.
- 570 United Nations: World Urbanization Prospects 2025 Summary of Results, 2025.
- Yang, Z. L., Niu, G. Y., Mitchell, K. E., Chen, F., Ek, M. B., Barlage, M., Longuevergne, L., Manning, K., Niyogi, D., Tewari, M., and Xia, Y.: The community Noah land surface model with multiparameterization options (Noah-MP): 2. Evaluation over global river basins, *Journal of Geophysical Research Atmospheres*, 116, <https://doi.org/10.1029/2010JD015140>, 2011.